

Amidinate–carboxylate complexes of dimolybdenum and ditungsten: $M_2(O_2CR)_2((N^iPr)_2CR')_2$. Preparations, molecular and electronic structures and reactions†‡§

Douglas J. Brown, Malcolm H. Chisholm* and Judith C. Gallucci

Received 4th October 2007, Accepted 24th January 2008

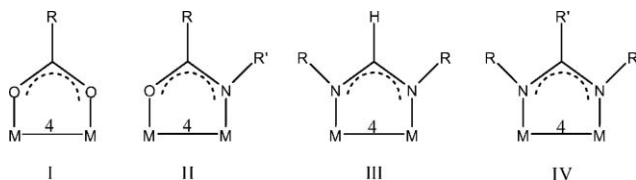
First published as an Advance Article on the web 22nd February 2008

DOI: 10.1039/b715258b

The compounds $M_2(O_2CMe)_4$ and the lithium amidinates $Li[(N^iPr)_2CR]$ react to give the new compounds $trans-M_2(O_2CMe)_2[(N^iPr)_2CR]_2$ where $M = Mo$ or W and $R = Me$ ($M = Mo$ only), $-C\equiv C^tBu$, $-C\equiv CPh$ and $-C\equiv C-Fc$ where $Fc = 1$ -ferrocenyl. The limitations of this type of reaction are described based on steric considerations together with the preparation and characterization of the compound $Mo_2(\mu-O_2C-9\text{-anthracene})_2[\eta^2-(N^iPr)_2CMe]_2$. The electronic structures of the bis-amidinate–bis-carboxylate M_2 complexes are described based on model compounds employing density functional theory and are correlated with the experimental observations of their physicochemical properties and in particular their observed electronic absorption spectra which show intense MLCT absorption bands. Preliminary studies of the reactions of these bis-amidinate–bis-carboxylate complexes in the preparation of 1-D oligomers are also described along with the preparation and molecular structures of the compounds $[Li(N^iPr)_2CR\cdot THF]_2$ where $R = 2$ -thienyl or $-C\equiv C-Ph$. The kinetic lability of these new M_2 -containing compounds toward ligand exchange is also noted.

Introduction

Compounds having MM quadruple bonds have been shown to have a rich and diverse coordination chemistry.¹ Bidentate ligands that can bridge the two metal atoms to form five-membered rings yield paddle-wheel type complexes, M_2L_4 , of which the group involving $L =$ carboxylate, amidate, formamidinate and amidinate shown in drawings I–IV, respectively, are prime examples.¹



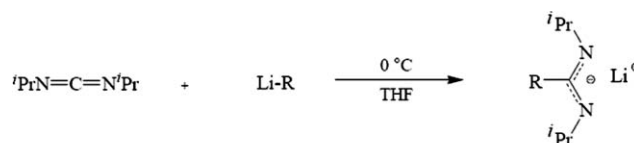
The carboxylate ligands are labile toward ligand exchange and this makes them ideal as starting materials for ligand exchange reactions. However, this can also form problems in syntheses where a kinetic product is desired.² The replacement of O by NR greatly reduces the facility of ligand scrambling and the Cotton group have used this to great effect in preparing dimers, molecular loops, triangles and squares with attendant formamidinate ligands.³ The formation of molecular loops, triangles and squares is greatly aided by the *cis*-templating unit $(ArNCHNAr)_2Mo_2^{2+}$

when used in conjunction with bridging dicarboxylate ligands. We were interested in the notion that the chemistry of amidinate complexes, $L =$ IV above, where the R group is bulky might act as *trans*-templating groups for $(RNC(R')NR)_2M_2^{2+}$ containing complexes ($M = Mo$ or W) and further that the introduction of certain R' groups might enter into $M_2(\delta)-R'(\pi)$ conjugation and thus complement earlier studies in this laboratory of $M_2(\delta)-L(\pi)$ conjugation employing $L =$ carboxylate.^{4,5} These ideas formed the platform upon which the work described herein was undertaken.

Results and discussion

Synthesis

Lithium amidinates were prepared from the reaction between a carbodiimide and an alkyllithium reagent as shown in Scheme 1.⁶



where $R = Me, C\equiv C^tBu, C\equiv CPh, C\equiv CFc, C_4H_4S$

Scheme 1 Synthesis of lithium amidinate salts.

In cases where an alkyllithium reagent was not commercially available it was prepared from the reaction between Bu^iLi and the alkyne or thiophene. In order to impart significant steric influence the carbodiimide was *N,N'*-diisopropyl. *N,N'*-Di-*tert*-butyl proved to be too demanding. The lithium amidinates formed large crystals upon cooling their THF solutions and two samples were examined crystallographically. The molecular structures

Department of Chemistry, The Ohio State University, Columbus, OH, 43210, USA

† Dedicated to Professor Ken Wade on the occasion of his 75th birthday.

‡ CCDC reference numbers 637924–637931. For crystallographic data in CIF or other electronic format see DOI: 10.1039/b715258b

§ Electronic supplementary information (ESI) available: Full crystallographic details; attempted synthesis of higher order oligomers. See DOI: 10.1039/b715258b

of $\text{Li}[(\text{N}^i\text{Pr})_2\text{CC}\equiv\text{CPh}]\cdot\text{THF}$ and $\text{Li}[(\text{N}^i\text{Pr})_2\text{C}-2-\text{C}_4\text{H}_8\text{S}]\cdot\text{THF}$ are shown in ESI,§ Fig. S1 and S2, respectively. In both instances there is a dimeric structure having a crystallographically imposed center of inversion. The lithium atoms are four coordinate in a pseudo-tetrahedral geometry. The amidinate ligands act as a chelating and bridging ligands as has been well documented and thus the molecular structures are not exceptional.⁷⁻⁹ The phenyl and thienyl rings are not contained in the amidinate NCN planes which limits the degree of π -conjugation of the thienyl unit and it is known that the presence of bulky R and R' in IV impede the ability of the amidinate ligand to bridge two metal centers and favor chelation as pictorially shown in Fig. 1. The challenge was then to select a series of amidinate ligands that would preferentially bridge the dimolybdenum or ditungsten units and to do this we employed R = *i*Pr and not *t*Bu and R' = Me and alkynyl derivatives. Other combinations proved problematic.

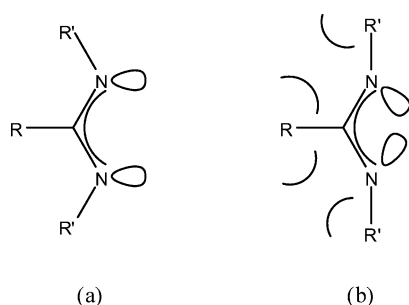
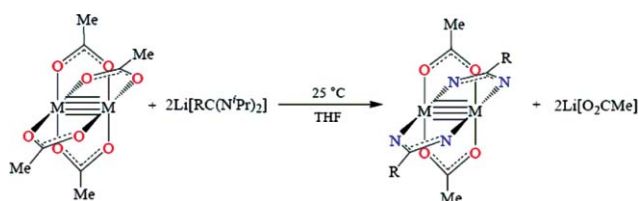


Fig. 1 (a) Bridging and (b) chelating modes of amidinates as influenced by steric factors.⁹

$\text{M}_2(\text{O}_2\text{CMe})_2[(\text{N}^i\text{Pr})_2\text{CR}]_2$ complexes

The new compounds were prepared according to the general reaction shown in Scheme 2, where M = Mo or W and R = Me (M = Mo only), $-\text{C}\equiv\text{C}^i\text{Bu}$, $-\text{C}\equiv\text{CPh}$ and $-\text{C}\equiv\text{CFc}$ (Fc = 1-ferrocenyl).



Isopropyl groups on amidinates omitted for clarity

Scheme 2 Synthesis of $\text{trans-M}_2(\text{O}_2\text{CCH}_3)_2[(\text{N}^i\text{Pr})_2\text{CR}]_2$.

The sparingly soluble, yellow $\text{M}_2(\text{O}_2\text{CMe})_4$ compounds and the lithium amidinates react with a color change and the visible formation of a white precipitate of LiO_2CMe . The reactions were allowed to proceed for several hours before the solvent was removed under a dynamic vacuum. The dried product was then extracted with CH_2Cl_2 and filtered over Celite to remove the lithium salt and the filtrate was collected and reduced in volume. Addition of ethanol to this filtrate induced the formation of a colored finely-divided microcrystalline product which was collected by filtration and dried in vacuum. The compounds were air- and moisture-sensitive and the tungsten complexes were the more sensitive. Prolonged

exposure to ethanol for the W_2 -containing species was avoided since this resulted in decomposition.

The compounds gave molecular ions by matrix assisted laser desorption ionization time of flight (MALDI-TOF) mass spectrometry. The ^1H NMR spectra revealed the presence of 1 : 1 carboxylate to amidinate ligands and significantly the isopropylmethyl groups appeared as a single doublet due to CH to Me proton coupling. This lack of diastereotopism implies a mirror plane of molecular symmetry and a *trans* arrangement of ligands. We propose that this geometry is favored by steric factors and further note that the product shown in Scheme 2 is favored even when 4 equiv. of the lithium amidinate is allowed to react with $\text{M}_2(\text{O}_2\text{CMe})_4$. The bis-bis products are thus the kinetically or thermodynamically favored compounds, when the bulky isopropyl groups are employed on the amidinate. With less bulky substituents such as the dimethylbenzylamidinate (DMBA) in the reaction with $\text{Mo}_2(\text{O}_2\text{CMe})_4$ the tetrasubstituted homoleptic compound $\text{Mo}_2(\text{DMBA})_4$ was isolated.

The reactions involving other $\text{Mo}_2(\text{O}_2\text{CR})_4$ compounds and $\text{Li}[(\text{N}^i\text{Pr})_2(\text{CR}')]_2$ compounds were also investigated (R' = Me). When R = *t*Bu the reaction proceeded but was complicated by the fact that the $\text{LiO}_2\text{C}^i\text{Bu}$ product was soluble and thus led to difficult purification of the desired bis-bis product. These reactions were not pursued further. The reactions between the $\text{Mo}_2(\text{O}_2\text{CR})_4$ compounds where R = 2-thienyl and 9-anthracenyl were also investigated and resulted in the formation of $\text{Mo}_2(\text{O}_2\text{CR})_2[(\text{N}^i\text{Pr})_2\text{CMe}]_2$. The 2-thienyl complex had the anticipated structure but the 9-anthracenyl derivative adopted an alternate *cis-cis* structure, *vide infra*, wherein the isopropylmethyl groups were diastereotopic (NMR).

For the sake of brevity the compounds of general formula and *trans*-geometry $\text{M}_2(\text{O}_2\text{CMe})_2[(\text{N}^i\text{Pr})_2\text{CR}]_2$ are referred to either as **A** or **B** for M = Mo or W, respectively and given the number **1**, **2**, **3** and **4** for R = Me, $-\text{C}\equiv\text{C}^i\text{Bu}$, $-\text{C}\equiv\text{CPh}$ and $-\text{C}\equiv\text{CFc}$, respectively.

Electronic structure calculations

Calculations employing density functional theory with the aid of the Gaussian 03 suite of programs were performed on model compounds for **1A**, **2A** and **3A** where the isopropyl group was substituted by a hydrogen atom (see Experimental section). This increased the symmetry and decreased computational time to achieve a set of self-consistent results that were verified to be a minimum on the potential energy surface. Molecular orbital analysis was used to verify the character of the individual orbitals as has been routinely applied in related studies of M_2 carboxylates and their derivatives.^{4,10} The replacement of the carboxylate group by the amidinates is similar to that of the substitution by a formamidinate in raising the orbital energy of the $\text{M}_2\delta$ orbital. Experimentally this results in lowering the electrochemical oxidation potential and in the gas phase the first ionization potential of the molecule.¹¹ However, more pertinent to this work is the nature of the ligand based π^* orbitals which in the amidinates where the R' group is unsaturated provide for a low energy MLCT absorption. For the compounds *trans*-bis carboxylate bis amidinate there are three ligand based π^* MOs of significance in the frontier orbital region. One is strictly O_2C based, another N_2C and the third is an admixture of the two. For the model compound of **1A**, where R = Me, these three π^* orbitals

are close in energy but with increasing conjugation as in **2A** ($R = -C\equiv C'Bu$) and **3A** ($R = -C\equiv CPh$) the amidinate π^* orbital drops in energy. This is schematically shown in Fig. 2. The time dependent DFT calculations on the model compounds for **1A**, **2A** and **3A** predict two relatively high energy absorptions, 310–340 nm, for the $M_2(\delta)$ to $CO_2(\pi^*)$ and the amidinate-carboxylate π^* orbital that remain fairly constant for the series but that the $M_2(\delta)$ to amidinate π^* transition moves to lower energy, e.g. 509 nm, for phenylacetylide complex.

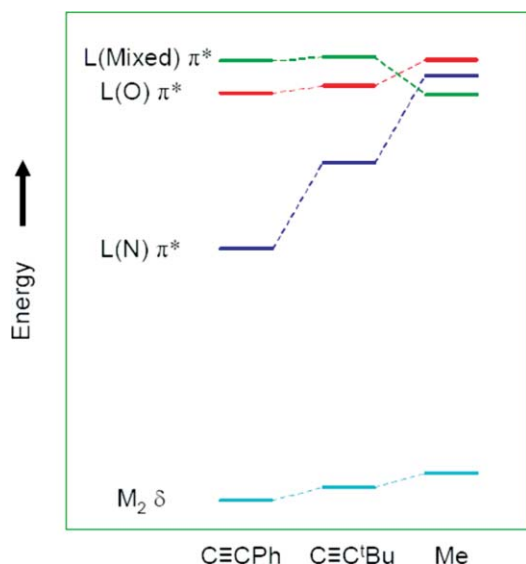


Fig. 2 Relative molecular orbital energies of $M_2(\delta)$ and ligand-based π^* in model complexes.

Electronic absorption spectra

All the new compounds are colored as a result of fully allowed metal-to-ligand charge transfer bands that occur in the visible region of the spectrum and mask the otherwise weak $M_2(\delta \rightarrow \delta^*)$ transition that is anticipated around 400 nm. A comparison of the molybdenum complexes, **1A**, **2A** and **3A** is shown in Fig. 3. The high energy absorptions below 300 nm are assigned to ligand π to π^* transitions. The spectrum of **1A** shows absorption in the region 300–350 nm which we assign to the three close in energy MLCT bands predicted according to the energy diagram shown in Fig. 4.

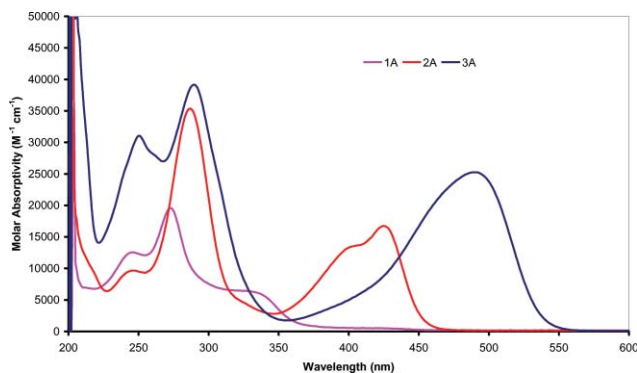


Fig. 3 UV-vis spectra of $Mo_2(O_2CCH_3)_2((N'Pr)_2CMe)_2$ (**1A**, magenta), $Mo_2(O_2CCH_3)_2((N'Pr)_2CC\equiv C'Bu)_2$ (**2A**, red), and $Mo_2(O_2CCH_3)_2((N'Pr)_2CC\equiv CPh)_2$ (**3A**, blue) complexes in THF at room temperature.

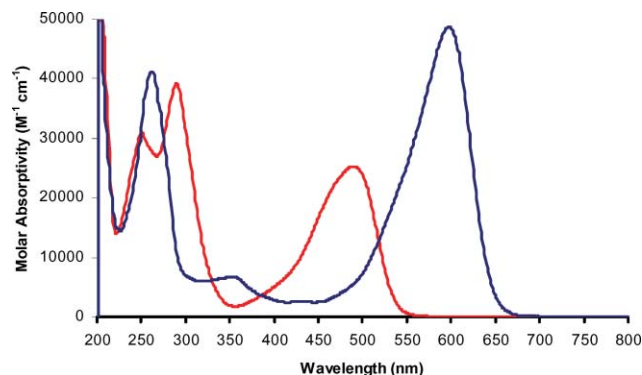


Fig. 4 UV-vis spectra of $M_2(O_2CCH_3)_2((N'Pr)_2CC\equiv CPh)_2$ where $M = Mo$ (red, **3A**) and $M = W$ (blue, **3B**) in THF at room temperature.

A very weak absorption around 420 nm could be the $MO_2(\delta \rightarrow \delta^*)$ transition. The spectra of the complexes **2A** and **3A** show lower energy and more intense absorptions which we assign to the MLCT bands involving the amidinate π^* orbitals as predicted by the frontier MO diagram shown in Fig. 2. The asymmetric nature of this absorption with the strong tailing effect to higher energy (shorter wavelength) may well be a result of overlapping and unresolved vibronic progressions. These do not, however, show significant sharpening on cooling in 2-MeTHF solutions.

The spectral features of the tungsten complexes are complementary and are red shifted as a result of the higher energy of the $W_2(\delta)$ orbital. A comparison of the absorption spectra of the complexes **3A** and **3B** is shown in Fig. 4. The blue color of the tungsten complex arises for the intense MLCT ($W_2(\delta)$ to amidinate π^*) absorption at 600 nm.

Electrochemistry

The new compounds were studied by cyclic voltammetry, CV, and normalized DPV curves for the complexes **1A**, **2A**, **2B**, **3A** and **3D** are shown in Fig. 5. It is clear that the ease of oxidation of the $M_2(\delta)$ orbital is sensitive to both the amidinate substituents, R' , and the metal as has been seen before.¹ The π -conjugation of the amidinates with the $M_2(\delta)$ orbital stabilizes the δ orbital

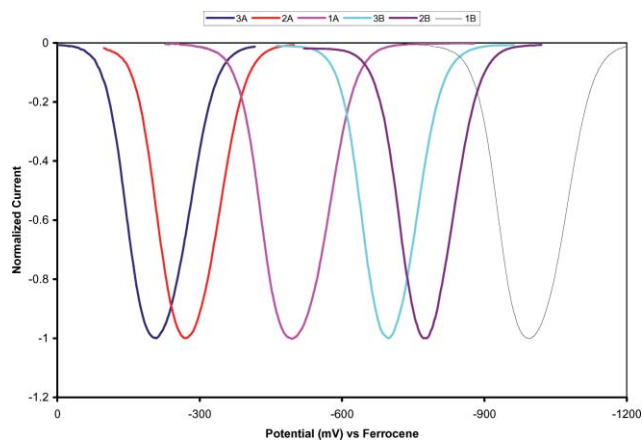


Fig. 5 Normalized differential pulse voltammograms of synthesized complexes and estimated voltammogram for complex **1B** in THF-0.1 M $[tBu_4N][PF_6]$ and referenced to $FeCp_2^{0/+}$ couple.

such that the ease of oxidation follows the order $R' = \text{Me} > -\text{C}\equiv\text{C}'\text{Bu} > -\text{C}\equiv\text{CPh}$. The related tungsten complexes are easier to oxidize by *ca.* 0.5 V which is typically seen for related $\text{M}_2(\text{O}_2\text{CR})_4$ compounds;¹² these in turn are more difficult to oxidize than the bis-acetate-bis-amidinate complexes reported here. For reasons which are unknown at this time we have not been able to make the tungsten analog of **1A**. Based on the oxidation trends shown in Fig. 5 we show the anticipated oxidation at -1.0 V vs. the $\text{Cp}_2\text{Fe}^{0/+}$ couple.

The ethynylferrocenyl amidinates, compounds **4A** and **4B** warrant specific attention since not only are the M_2 centers redox active but so too are the ferrocenyl units which could be electronically coupled through $\text{M}_2(\delta)$ -ligand π -conjugation.

The CV and DPV for the molybdenum complex **4A** are shown in Fig. 6. The first oxidation wave at -308 mV corresponds to oxidation of the $\text{Mo}_2(\delta)$ orbital and is comparable to that observed for compounds **2A** and **3A**. The second oxidation at $\sim +0.1$ V corresponds to a two-electron oxidation wave and involves oxidation of the ferrocenyl units. The appearance of a single wave indicates that the two Cp_2Fe units are not significantly coupled through the Mo_2 center. A similar situation pertains to the tungsten complex **4B**, where the W_2 oxidation occurs at -778 mV. The lack of electronic coupling of the two Cp_2Fe centers at a distance of *ca.* 16.5 Å, *vide infra*, is perhaps not surprising although we do note that Ren and co-workers¹³ have seen significant coupling in related Ru_2 containing systems with axially aligned alkynyl Cp_2Fe units.

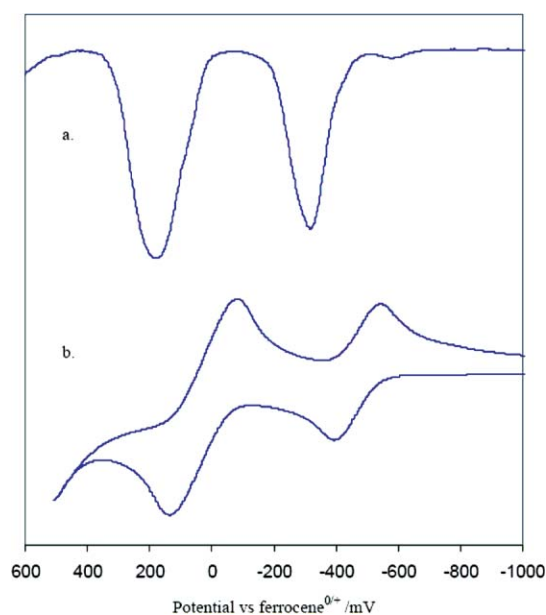


Fig. 6 (a) Differential pulse voltammogram and (b) cyclic voltammogram of $\text{Mo}_2(\text{O}_2\text{CCH}_3)_2((i\text{PrN})_2\text{CC}\equiv\text{CFC})_2$ (**4A**) in THF-0.1 M [$t\text{Bu}_4\text{N}$][PF_6].

Single-crystal and molecular structures

The new compounds were readily crystallized from routine organic solvents and three compounds were subjected to single-crystal X-ray determinations. The molecular structure of the compound **1A** is shown in Fig. 7. The expected paddle-wheel structure is seen with the *trans* disposition of ligands. The molecule has a

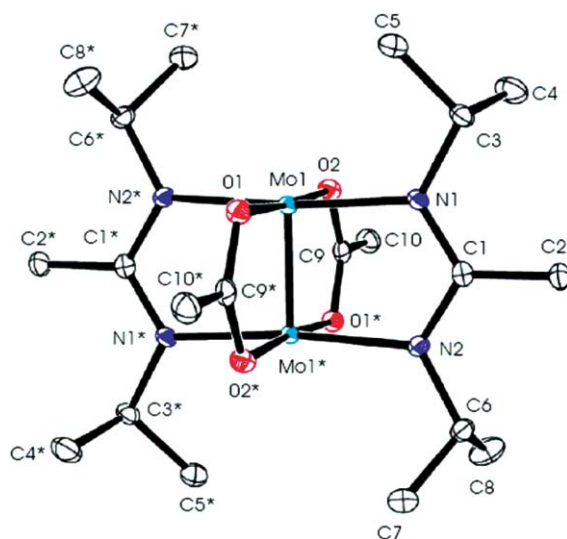


Fig. 7 ORTEP diagram of the centrosymmetric $\text{Mo}_2(\text{O}_2\text{CCH}_3)_2((\text{N}^i\text{Pr})_2\text{-CMe})_2$ molecule (**1A**) drawn with 50% probability displacement ellipsoids. Hydrogen atoms are omitted for clarity. The starred atoms (*) are related to the corresponding unstarred atom by the crystallographic inversion center. The Mo–Mo, Mo–O(carboxylate), and Mo–N(amidinate) interatomic distances are 2.0691(2), 2.1239(11)–2.1435(11), and 2.1371(13)–2.1419(13) Å, respectively.

crystallographically imposed center of inversion and the bulky $i\text{Pr}$ groups are oriented away or distal to the MoMo bond.

The molecular structure of the tungsten complex **3B**, is shown in Fig. 8. There is again a similar *trans* disposition of ligands in the centrosymmetric structure with a similar arrangement of the $i\text{Pr}$ groups. The phenyl groups are nearly coplanar with the amidinate N_2C units.

The molecular structure of the ferrocenyl complex **4A** is shown in Fig. 9. The similarity of the fundamental structural features of these compounds is quite striking, but otherwise not exceptional for MM quadruply bonded paddle-wheel complexes.

In contrast, the molecular structure of the $\text{Mo}_2((\text{N}^i\text{Pr})_2\text{CMe})_2-(\text{O}_2\text{C-9-anthracene})_2$ shown in Fig. 10 reveals a totally different mode of bonding. The two carboxylate ligands are *cis* and the amidinates are chelating to each metal center. As noted in Fig. 3, the chelating nature of the amidinate ligand is favored by the introduction of bulky groups on the central carbon atom. In the present case, however, it is most likely that the observed structure (Fig. 10) is a result of competing steric factors. The *peri* $\text{CH}\cdots\text{O}$ interactions of 9-anthracene carboxylate ligands and esters favor a dihedral angle of $\sim 56^\circ$ between the aromatic ring and the CO_2 moiety.^{14,15} Indeed, earlier calculations on 9,10-anthracene dicarboxylate bridged Mo_4 containing compounds predict that the planar structure where the dihedral angle is zero is 11 kcal mol^{-1} higher in energy.¹⁶ Thus, for a *trans,trans*-bridged amidinate structure of the type seen for the other new compounds described herein we would anticipate a significant steric repulsion between the anthracene ring and the isopropyl groups which are distal to the MM bond. As can be seen from the view of the molecule shown in Fig. 10 this type of steric repulsion is avoided with the *cis*-chelating structure.

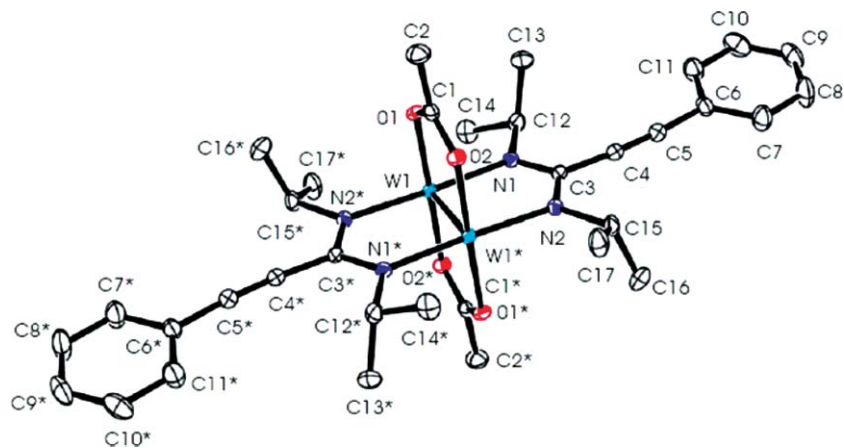


Fig. 8 ORTEP diagram of the centrosymmetric $W_2(O_2CCH_3)_2((N^iPr)_2CC\equiv CPh)_2$ molecule (**3B**) drawn with 50% probability displacement ellipsoids. Hydrogen atoms are omitted for clarity. The starred atoms (*) are related to the corresponding unstarred atom by the crystallographic inversion center. The W–W, W–O(carboxylate) and W–N(amidinate) interatomic distances are 2.17294(17), 2.1004(16)–2.1056(17) and 2.100(2)–2.104(2) Å, respectively. The dihedral angle between the phenyl ring and its amidinate group is 9.0° .

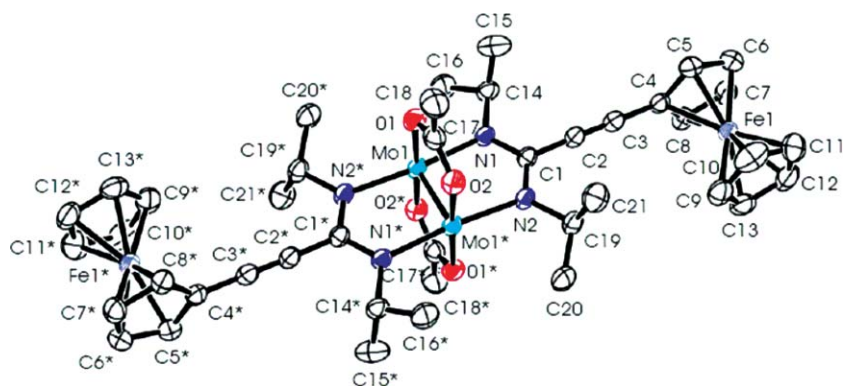


Fig. 9 ORTEP diagram of the centrosymmetric $Mo_2(O_2CCH_3)_2((N^iPr)_2CC\equiv CFc)_2$ molecule (**4A**) drawn with 50% probability displacement ellipsoids. Hydrogen atoms are omitted for clarity. The starred atoms (*) are related to the corresponding unstarred atom by the crystallographic inversion center. The Mo–Mo, Mo–O(carboxylate), and W–N(amidinate) interatomic distances are 2.0779(4), 2.126(2)–2.128(2) and 2.117(2)–2.125(2) Å, respectively. The dihedral angle between cyclopentadienyl ring and its amidinate group is 91.3° .

Ligand scrambling reactions

As noted earlier ligand scrambling reactions are facile for $M_2(O_2CR)_4$ compounds and can be catalyzed by either the presence of trace amounts of free carboxylic acid or the carboxylate anion.² The introduction of the amidinates was expected to impart greater kinetic persistence and in order to evaluate whether this was indeed the case the reaction between $Mo_2(O_2CCF_3)_4$ and $Mo_2(O_2CMe)_2[(N^iPr)_2CC\equiv C^iBu]_2$, **2A**, was monitored. These two compounds were selected because of their similar solubility. An equimolar mixture of the two compounds was dissolved in benzene- d_6 and placed in a J. Young[®] NMR tube under an N_2 atmosphere. The reaction was monitored with time by both 1H NMR spectroscopy and mass spectrometry.

At room temperature the 1H signals of the acetate ligands were most informative. Within 6 h the appearance of two new acetate 1H signals was detectable and these could be assigned to the products of acetate–trifluoroacetate ligand exchange, namely $Mo_2[(N^iPr)_2CMe]_2(O_2CMe)(O_2CCF_3)$ and $Mo_2(O_2CCF_3)_3(O_2CMe)$. Within 3 days at room temperature the major acetate signal was still due to **2A** but additional

acetate signals were present, most likely due to *cis* and *trans* $Mo_2(O_2CMe)_2(O_2CCF_3)_2$. After 3 days the sample was heated to $+70^\circ C$ for 3 h and by 1H NMR spectroscopy at least eleven acetate methyl signals could be seen along with a significant loss of the signal due to **2A**. The MALDI-TOF mass spectrum of the mixture formed after heating for 3 h was also recorded. As shown in Fig. 11, ions arising from acetate–trifluoroacetate and amidinate–trifluoroacetate exchange were observed. We can therefore conclude that the amidinate ligands, though relatively less labile than the carboxylates in solution at room temperature, are still kinetically labile to ligand scrambling, especially upon heating in solution.

Higher-order oligomers

The unique *trans–trans* geometry of the mixed acetate amidinate complexes led us to investigate their potential in the synthesis of 1-D polymeric chains based on the replacement of the acetate ligands by dicarboxylate ligands.¹⁷ Schematically the reaction can

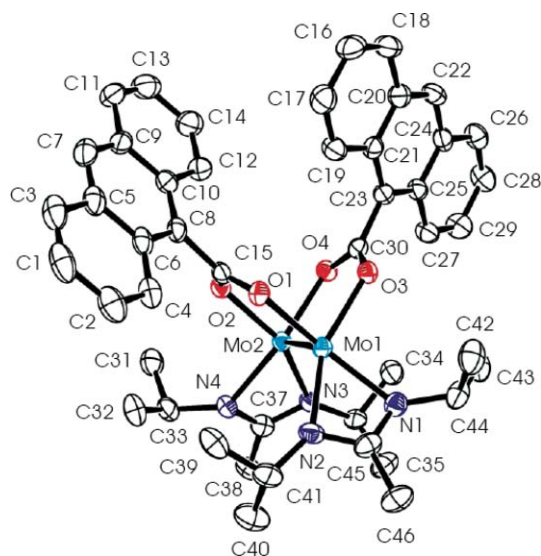


Fig. 10 ORTEP diagram of $\text{Mo}_2(\text{cis-}\mu\text{-O}_2\text{C-9-anthracene})_2(\eta^2\text{-}(\text{N}'\text{Pr})_2\text{CMe})_2$ molecule drawn with 50% probability displacement ellipsoids. Hydrogen atoms are omitted for clarity. The Mo–Mo, Mo–O(carboxylate), and M–N(amidinate) interatomic distances are 2.1308(4), 2.096(2)–2.117(2) and 2.156(3)–2.165(3) Å, respectively. The dihedral angle between anthracene ring and its carboxylate group is 76.5–63.9°.

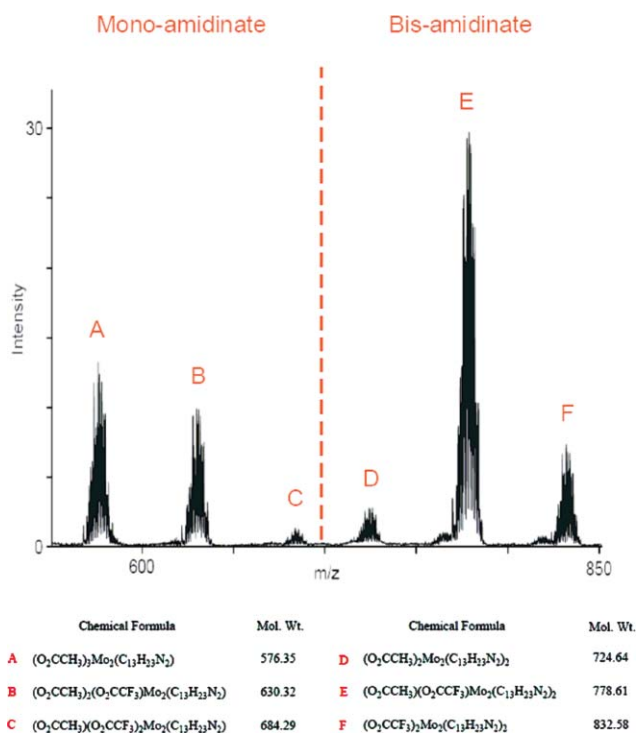
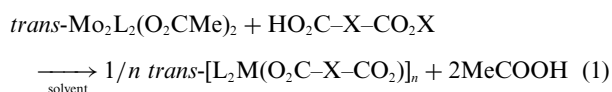


Fig. 11 MALDI-TOF mass spectra of the ligand scrambling reaction involving **2A** and $\text{Mo}_2(\text{O}_2\text{CCF}_3)_4$ upon heating at approximately 70 °C for 3 h. The chemical formula and molecular weights of identified species are labeled.

be represented by eqn (1).



The reactions were run in various solvents (THF, hexanes, EtOH) for periods of 14–21 days. As a prototypical bridge we employed the use of 1,4-terephthalate ($\text{X} = \text{C}_6\text{H}_4$). The products in these reactions were not easy to characterize as “polymers” but rather are formulated as a mixture of relatively short chain oligomers having terminal O_2CMe and $\text{O}_2\text{CC}_6\text{H}_4\text{COOH}$ groups *e.g.* $(\text{MeCO}_2)_2\text{L}_2\text{Mo}_2\text{O}_2\text{CC}_6\text{H}_4\text{CO}_2\text{Mo}_2\text{L}_2(\text{O}_2\text{CMe})$ and $(\text{MeCO}_2)\text{-L}_2\text{Mo}_2(\text{O}_2\text{CC}_6\text{H}_4\text{CO}_2)\text{Mo}_2\text{L}_2(\text{O}_2\text{CC}_6\text{H}_4\text{CO}_2)\text{Mo}_2\text{L}(\text{O}_2\text{CMe})$ based on MALDI-TOF mass spectrometry, where $\text{L} = (\text{N}'\text{Pr})_2\text{CC}\equiv\text{CPh}$.

In an attempt to prepare 1-D polymers by a salt metathesis reaction involving a cationic complex $\text{Mo}_2[(\text{N}'\text{Pr})_2\text{CC}\equiv\text{CPh}]_2(\text{CH}_3\text{CN})_4^{2+}[\text{BF}_4^-]_2$ and the dicarboxylate anion $[\text{O}_2\text{C-X-CO}_2]^{2-}$, the reaction between **2A** and Et_3OBF_4 (2 equiv.) in CH_3CN was investigated. However, this did not lead to the desired bisamidinate cationic complex but rather the cation $\text{Mo}_2[(\text{N}'\text{Pr})_2\text{CC}\equiv\text{CPh}](\text{O}_2\text{CMe})(\text{CH}_3\text{CN})_x^{2+}$ by replacement of both acetate and amidinate ligands. This approach was thus not pursued further.

These reactions aimed at preparing higher order oligomers and described in the ESI.†

Concluding remarks

This work has allowed for the synthesis and characterization of a new series of mixed amidinate–carboxylates of dimolybdenum and ditungsten, $\text{M}\equiv\text{M}$. Though interesting in their own right, these complexes still suffer from kinetic lability toward ligand exchange reactions and have not proved useful in the synthesis of 1-D polymers, which has been a topic of some interest to this group for some time.^{17,18}

Experimental

Physical measurements

NMR spectra were recorded on a 400 MHz Bruker DPX Avance400 spectrometer. All ^1H NMR chemical shifts are reported in ppm relative to the protio impurity in $\text{THF-}d_8$ at 3.58 ppm or benzene- d_6 at 7.15 ppm from a 90% benzene–10% THF mixture by weight. Electronic spectra at room temperature were recorded by using a Perkin-Elmer Lambda 900 spectrometer in THF solution. Microanalyses were carried out by Atlantic Microlab, Inc. Cyclic voltammetric and differential pulse voltammetric data were collected with the aid of a Princeton Applied Research (PAR) 173A potentiostat-galvanostat equipped with a PAR 176 current-to-voltage converter with *iR* compensation capability. A single compartment voltammetric cell was equipped with a platinum working electrode, a platinum wire auxiliary electrode, and a pseudo-reference electrode consisting of a silver wire in 0.5 M $^n\text{Bu}_4\text{NPF}_6\text{-THF}$ separated from the bulk solution by a Vycor tip. Ferrocene was added as an internal reference and typically was found at +0.75 V under these conditions.

Synthesis

All reactions were carried out under an atmosphere of oxygen-free UHP-grade argon using standard Schlenk techniques or under a dry and oxygen-free nitrogen atmosphere using standard glovebox techniques. All solvents were dried and degassed

by standard methods and distilled prior to use. Dimolybdenum tetraacetate, $\text{Mo}_2(\text{O}_2\text{CMe})_4$,¹⁹ and ditungsten tetraacetate, $\text{W}_2(\text{O}_2\text{CMe})_4$,²⁰ were prepared according to the literature procedures. *N,N'*-Diisopropylcarbodiimide, *tert*-butylacetylene, *n*-butyllithium (2.5 M in hexanes), methyllithium (1.6 M in diethyl ether), lithium phenylacetylide (1.0 M in THF), terephthalic acid, and 2,5-thiophenedicarboxylic acid were purchased from commercial sources and used as received.

Preparation of $\text{Li}[(\text{N}^i\text{Pr})_2\text{CC}\equiv\text{CPh}]$

1.25 mL of *N,N'*-diisopropylcarbodiimide (8.0 mmol) was dissolved in approximately 25 mL of THF and cooled to 0 °C. 5 mL of 1.6 M methyllithium (8.0 mmol) in THF was added to the mixture. The solution was allowed to warm slowly to room temperature. After 2 h, the solvent was evaporated to dryness under a dynamic vacuum to give a tan solid in quantitative yield.

Preparation of $\text{Li}[(\text{N}^i\text{Pr})_2\text{CC}_4\text{H}_4\text{S}]$

2.0 mL of thiophene (10.0 mmol) was dissolved in approximately 25 mL of THF and cooled to 0 °C. 10 mL of 1.0 M *n*-butyllithium (10.0 mmol) in THF was added to the mixture. The solution was allowed to warm slowly to room temperature. After 2 h, the solution was again cooled to 0 °C and 3.9 mL of *N,N'*-diisopropylcarbodiimide was slowly added to the mixture and allowed to warm to room temperature.

Preparation of $\text{Mo}_2(\text{O}_2\text{CMe})_2(\text{N}^i\text{Pr})_2\text{CMe}_2$ (1A)

1.25 mL of *N,N'*-diisopropylcarbodiimide (8.0 mmol) was dissolved in approximately 25 mL of THF and cooled to 0 °C. 5 mL of 1.6 M methyllithium (8.0 mmol) in THF was added to the mixture. The solution was allowed to warm slowly to room temperature. After 2 h, it was used *in situ* for the next reaction. A slurry of 1.72 g of $\text{Mo}_2(\text{O}_2\text{CMe})_4$ (4.0 mmol) in approximately 25 mL of THF was cooled to 0 °C. The *in situ* solution was cooled again to 0 °C and slowly added to the slurry. The initial color change was red but darkened with time. After stirring at room temperature overnight, the mixture was evaporated to dryness under a dynamic vacuum and redissolved in approximately 50 mL of dichloromethane. The solution was filtered over Celite. The volume of the red solution was reduced to a minimum (~3 mL) and ethanol (~5 mL) was added to precipitate the product. The yellow product was collected on a glass frit, washed with 10 mL of ethanol, and yielded 825 mg. The filtrate was evaporated to dryness and 10 mL of ethanol was added. This resulted in a yellow suspension. The solid was washed three times with approximately 10 mL of ethanol and allowed to settle (each time the supernatant liquid was cannulated off). The remaining solid was dried and yielded a second crop 500 mg. Overall yield: 1.325 g (55.9%).

Microanalysis: found: C 40.22; H 6.67; N 9.18%. $\text{C}_{20}\text{H}_{40}\text{N}_4\text{O}_4\text{Mo}_2$ requires: C 40.55; H 6.81; N 9.46%. NMR (benzene-*d*₆): ¹H (400 MHz) 4.19 (septet, $J_{\text{HH}} = 6.4$ Hz, 4H, *CHMe*₂), 2.32 (s, 6H, *CMe*), 2.21 (s, 6H, *CMe*), 0.92 (d, $J_{\text{HH}} = 6.4$ Hz, 24H, *CHMe*₂). The methyl groups of the acetate and amidinate have not been assigned. MALDI-MS: 593.1 (100%, M⁺).

Attempted preparation of $\text{W}_2(\text{O}_2\text{CCH}_3)_2(\text{N}^i\text{Pr})_2\text{CMe}_2$ (1B)

The reaction was carried out under similar conditions outlined for the molybdenum analogue by using 600 mg of $\text{W}_2(\text{O}_2\text{CCH}_3)_4$ (1.0 mmol), 0.31 mL of *N,N'*-diisopropylcarbodiimide (2.0 mmol) and 1.25 mL of 1.6 M methyllithium (2.0 mmol). Within minutes, the solution turned gray. After 2 h, the solvent was removed under a dynamic vacuum but the mixture yielded no tractable product.

$\text{Mo}_2(\text{O}_2\text{CMe})_2(\text{N}^i\text{Pr})_2\text{CC}\equiv\text{C}^i\text{Bu}$ (2A)

3.2 mL of 2.5 M *n*-butyllithium (8.0 mmol) was slowly added a mixture of 1 mL of *tert*-butylacetylene (8.0 mmol) in 25 mL of THF at -78 °C. The solution was allowed to stir at room temperature for 2 h. The solution appeared almost colorless. It was used *in situ* for the next reaction. 1.25 mL of *N,N'*-diisopropylcarbodiimide (8.0 mmol) was slowly added to the *in situ* mixture at 0 °C. The solution was allowed to stir at room temperature for 2 h. The solution appeared colorless. It was used *in situ* for the next reaction. A slurry containing 1.72 g of $\text{Mo}_2(\text{O}_2\text{CMe})_4$ in 25 mL of THF was cooled to 0 °C. The *in situ* amidinate salt was cooled again to 0 °C and slowly added to the slurry. The solution rapidly turned red. Within the first hour the solution was dark. After stirring overnight, the solvent was removed under a dynamic vacuum and the residue was redissolved in approximately 50 mL of CH_2Cl_2 . The solution was filtered over Celite. The volume of the solution was reduced to a minimum by a dynamic vacuum and ethanol was added to precipitate the product. The solid was collected by using a glass frit and washed with 2 × 10 mL of hexanes. The yield was 810 mg. The filtrate was evaporated to dryness and redissolved in pure ethanol. The second crop of product was collected using a glass frit and yielded 220 mg. Overall yield: 1.030 g (35.5%).

Microanalysis: found: C 49.12; H 7.26; N 7.65%. $\text{C}_{30}\text{H}_{52}\text{N}_4\text{O}_4\text{Mo}_2$ requires: C 49.72; H 7.23; N 7.73%. NMR (benzene-*d*₆): ¹H (400 MHz) 4.90 (septet, $J_{\text{HH}} = 6.5$ Hz, 4H, *CHMe*₂), 2.23 (s, 6H, *O}_2\text{CMe}*), 1.19 (s, 18H, *CMe*₃) 1.10 (d, $J_{\text{HH}} = 6.5$ Hz, 24H, *CHMe*₂). MALDI-MS: 724.2 (100%, M⁺).

$\text{W}_2(\text{O}_2\text{CMe})_2(\text{N}^i\text{Pr})_2\text{CC}\equiv\text{C}^i\text{Bu}$ (2B)

The reaction was carried out under similar conditions outlined for the molybdenum analogue using 600 mg of $\text{W}_2(\text{O}_2\text{CMe})_4$ (1.0 mmol), 0.8 mL of 2.5M *n*-butyllithium (2.0 mmol), 0.25 mL of *tert*-butylacetylene (8.0 mmol), and 0.31 mL of *N,N'*-diisopropylcarbodiimide (2.0 mmol). An orange solid (310 mg, 34.3% yield) was isolated by filtration.

NMR (benzene-*d*₆): ¹H (400 MHz) 5.16 (septet, $J_{\text{HH}} = 6.5$ Hz, 4H, *CHMe*₂), 2.44 (s, 6H, *O}_2\text{CMe}*), 1.23 (s, 18H, *CMe*₃) 1.20 (d, $J_{\text{HH}} = 6.5$ Hz, 24H, *CHMe*₂). MALDI-MS: 900.3 (100%, M⁺).

$\text{Mo}_2(\text{O}_2\text{CMe})_2(\text{N}^i\text{Pr})_2\text{CC}\equiv\text{CPh}$ (3A)

1.25 mL of *N,N'*-diisopropylcarbodiimide (8.0 mmol) was dissolved in 25 mL of THF and cooled to 0 °C. 8.0 mL of 1 M lithium phenylacetylide (8.0 mmol) was added to the mixture. The solution was allowed to warm slowly to room temperature. After 2 h, it was used *in situ* for the next reaction. A slurry of 1.72 g of $\text{Mo}_2(\text{O}_2\text{CMe})_4$ in 25 mL of THF was made and cooled to 0 °C. The *in situ* solution was cooled again to 0 °C and slowly added to the slurry. The initial color was red but darkened with

reaction time. After stirring at room temperature overnight, the solvent was evaporated to dryness and the residue was redissolved in approximately 50 mL of dichloromethane. The solution was filtered over Celite. The volume of the red solution was reduced to a minimum and ethanol was added to precipitate the product. The product was collected on a glass frit, washed with 10 mL of ethanol, yielding 1.85 g. The filtrate was evaporated to dryness and 10 mL of ethanol was added. This resulted in an orange suspension. The solid was collected by filtration and was washed three times with approximately 10 mL of ethanol and allowed to settle (each time the supernatant liquid was cannulated off). The remaining solid was dried and yielded a second crop 0.5 g. Overall yield: 2.35 g (76.8%).

Microanalysis: found: C 51.52; H 5.63; N 6.74%. $C_{34}H_{44}N_4O_4Mo_2$ requires: C 53.41; H 5.80; N 7.33%. NMR (benzene- d_6): 1H (400 MHz) 7.56 (m, 4H, phenyl H), 7.37 (m, 6H, phenyl H), 4.77 (septet, $J_{HH} = 6.5$ Hz, 4H, $CHMe_2$), 2.39 (s, 6H, O_2CMe), 0.90 (d, $J_{HH} = 6.5$ Hz, 24H, $CHMe_2$). MALDI-MS: 765.2 (100%, M^+).

$W_2(O_2CMe)_2((N^iPr)_2CC\equiv CPh)_2$ (3B)

The reaction was carried out under similar conditions outlined for the molybdenum analogue by using 604 mg of $W_2(O_2CMe)_4$ (1.0 mmol), 0.31 mL of N,N' -diisopropylcarbodiimide (2.0 mmol) and 2.0 mL of 1.0 M lithium phenylacetylide (2.0 mmol). A single crop of blue solid (0.340 g, 36.2% yield) was collected by filtration.

Microanalysis: found: C 42.65; H 4.70; N 5.90%. $C_{34}H_{44}N_4O_4W_2$ requires: C 43.42; H 4.72; N 5.96%. NMR (benzene- d_6): 1H (400 MHz) 7.38 (d, $J_{HH} = 7.4$ Hz, 4H, phenyl *o*-H), 7.05 (t, $J_{HH} = 7.6$ Hz, 4H, phenyl *m*-H), 6.93 (d, $J_{HH} = 7.5$ Hz, 2H, phenyl *p*-H), 5.30 (septet, $J_{HH} = 6.5$ Hz, 4H, $CHMe_2$), 2.45 (s, 6H, O_2CMe), 1.24 (d, $J_{HH} = 6.5$ Hz, 24H, $CHMe_2$). MALDI-MS: 940.2 (100%, M^+).

Preparation of $Mo_2(O_2CCH_3)_2((N^iPr)_2CC\equiv CFc)_2$ (4A)

0.8 mL of 2.5M *n*-butyllithium was slowly added to a mixture of 430 mg of ethynylferrocene in approximately 50 mL of THF at 0 °C. The solution was allowed to stir at room temperature for 2 h. It was used *in situ* for the next reaction. 0.31 mL of N,N' -diisopropylcarbodiimide was slowly added to the *in situ* mixture at 0 °C. The solution was allowed to stir at room temperature for 2 h. It was used *in situ* for the next reaction. A slurry containing 428 mg of $Mo_2(O_2CCH_3)_4$ in 25 mL of THF was cooled to 0 °C. The *in situ* solution was cooled again to 0 °C and slowly added to the slurry. The solution initially turned red. Within the first hour the solution darkened. After stirring overnight, the mixture was evaporated to dryness and redissolved in approximately 50 mL of CH_2Cl_2 . The solution was filtered over Celite. The volume of the solution was reduced to a minimum and the desired product precipitated. The orange solid was collected using a glass frit and washed with hexane. Overall yield: 385 mg (39.3%).

Microanalysis: found: C 51.53; H 5.29; N 5.69%. $C_{42}H_{52}N_4O_4Fe_2Mo_2$ requires: C 51.45; H 5.35; N 5.71%. NMR (benzene- d_6): 1H (400 MHz) 5.06 (septet, $J_{HH} = 6.4$ Hz, 4H, $CHMe_2$), 4.43 (s, 4H, Fc), 4.10 (s, 10H, Fc), 3.97 (s, 4H, Fc), 2.28 (s, 6H, O_2CMe), 1.16 (d, $J_{HH} = 6.4$ Hz, 24H, $CHMe_2$). MALDI-MS: 980.1 (100%, M^+).

Preparation of $W_2(O_2CCH_3)_2((N^iPr)_2CC\equiv CFc)_2$ (4B)

The reaction was carried out under similar conditions outlined for the molybdenum analogue by using 604 mg of $W_2(O_2CMe)_4$ (1.0 mmol), 430 mg of ethynylferrocene (2.0 mmol), 0.8 mL of 2.5 M *n*-butyllithium (2.0 mmol) and 0.31 mL of N,N' -diisopropylcarbodiimide (2.0 mmol). 280 mg of a dark red solid yield was isolated by filtration. The filtrate was stripped to dryness and redissolved in 10 mL of THF. This solution was placed in the -40 °C refrigerator to grow crystals. After several days, the mother-liquor was removed and a 100 mg crop of crystals was collected. Overall yield: 380 mg (32.9%).

Microanalysis: found: C 43.71; H 4.49; N 4.65%. $C_{42}H_{52}N_4O_4Fe_2W_2$ requires: C 43.63; H 4.53; N 4.85%. NMR (benzene- d_6): 1H (400 MHz) 5.33 (septet, $J_{HH} = 6.4$ Hz, 4H, $CHMe_2$), 4.39 (s, 4H, Fc), 4.09 (s, 10H, Fc), 3.98 (s, 4H, Fc), 2.45 (s, 6H, O_2CMe), 1.27 (d, $J_{HH} = 6.4$ Hz, 24H, $CHMe_2$). MALDI-MS: 1156.2 (100%, M^+).

Preparation of $Mo_2(O_2C-2-thiophene)_2((N^iPr)_2CMe)_2$

0.31 mL of N,N' -diisopropylcarbodiimide (2.0 mmol) was dissolved in 25 mL of THF and cooled to 0 °C. 1.25 mL of 1.6 M methyllithium (2.0 mmol) was added to the mixture. The solution was allowed to warm slowly to room temperature. After 2 h, it was used *in situ* for the next reaction. A slurry of 0.7 g of $Mo_2(O_2C-2-thiophene)_4$ ²¹ in 25 mL of THF was made and cooled to 0 °C. The *in situ* solution was cooled again to 0 °C and slowly added to the slurry. The initial color change was black but changed to a deep red. After stirring at room temperature for two days, the solvent was removed under a dynamic vacuum and the residue was redissolved in approximately 25 mL of CH_2Cl_2 . The solution was filtered over Celite. The volume of the red solution was reduced to a minimum to precipitate an orange-red solid. The product was collected on a glass frit and washed with 2 × 5 mL of hexanes. Additional hexanes were added to the filtrate which caused a second precipitation. This second batch was also collected on a frit and washed with 2 × 5 mL hexanes. The solid was dried under vacuum for several hours. Overall yield: 130 mg (17.9%).

NMR (benzene- d_6): 1H (400 MHz) 7.67 (d, 2H, thiophene), 6.79 (d, 2H, thiophene), 6.63 (t, 2H, thiophene), 4.16 (septet, 4H, $CHMe_2$), 2.01 (s, 6H, N_2CMe), 0.95 (d, 24H, $CHMe_2$). MALDI-MS: 728.1 (100%, M^+).

Preparation of $Mo_2(cis-\mu-O_2C-9-anthracene)_2(\eta^2-(N^iPr)_2CMe)_2$

0.31 mL of N,N' -diisopropylcarbodiimide (2.0 mmol) was dissolved in 25 mL of THF and cooled to 0 °C. 1.25 mL of 1.6 M methyllithium (2.0 mmol) was added to the mixture. The solution was allowed to warm slowly to room temperature. After 2 h, it was used *in situ* for the next reaction. A slurry of 1.08 g of $Mo_2(O_2C-9-anthracene)_4$ ¹⁴ in 25 mL of THF was made and cooled to 0 °C. The *in situ* solution was cooled again to 0 °C and slowly added to the slurry. The initial color changed to a deep red. After stirring at room temperature for two days, the solvent was removed under a dynamic vacuum and the residue was redissolved in approximately 25 mL of CH_2Cl_2 . The solution was filtered over Celite. The volume of the solution was reduced to a minimum and ethanol was added to precipitate a purple solid. The product was collected on a glass

Table 1 Crystallographic details and data collection for Li[(NⁱPr)₂CC≡CPh], Li[(NⁱPr)₂CC₄H₄S], Mo₂(O₂CCH₃)₂((NⁱPr)₂CMe)₂ **1A** and Mo₂(O₂CCH₃)₂((NⁱPr)₂CC≡CPh)₂·3thf **3A**

	Li[(N ⁱ Pr) ₂ CC≡CPh]	Li[(N ⁱ Pr) ₂ CC ₄ H ₄ S]	Mo ₂ (O ₂ CCH ₃) ₂ - ((N ⁱ Pr) ₂ CMe) ₂ 1A	Mo ₂ (O ₂ CCH ₃) ₂ ((N ⁱ Pr) ₂ CC≡CPh) ₂ ·3thf 3A
Formula	C ₃₈ H ₅₄ Li ₂ N ₄ O ₂	C ₁₅ H ₂₅ LiN ₂ OS	C ₂₀ H ₄₀ Mo ₂ N ₄ O ₄	C ₃₄ H ₄₄ Mo ₂ N ₄ O ₄ ·3C ₄ H ₈ O
<i>M_r</i>	612.73	288.37	592.44	980.92
Crystal system	Triclinic	Monoclinic	Triclinic	Triclinic
Space group	<i>P</i> $\bar{1}$	<i>P</i> 2 ₁ / <i>c</i>	<i>P</i> $\bar{1}$	<i>P</i> $\bar{1}$
<i>T</i> /K	200(2)	200(2)	200(2)	200(2)
<i>a</i> /Å	9.724(1)	9.173(1)	8.3023(10)	9.311(1)
<i>b</i> /Å	10.008(1)	10.970(1)	9.0596(10)	11.735(1)
<i>c</i> /Å	19.713(2)	17.190(2)	9.5252(10)	12.973(1)
<i>a</i> /°	93.575(5)		68.840(4)	66.083(3)
<i>β</i> /°	91.225(5)	95.953(7)	77.080(4)	74.895(3)
<i>γ</i> /°	90.848(4)		65.805(5)	68.780(5)
<i>V</i> /Å ³	1914.0(3)	1720.5(3)	607.03(12)	1197.1(2)
<i>Z</i>	2	4	1	1
<i>D_c</i> /g cm ⁻³	1.063	1.113	1.621	1.361
<i>F</i> (000)	664	624	304	512
<i>λ</i> (Mo-Kα)/Å	0.71073	0.71073	0.71073	0.71073
<i>μ</i> /mm ⁻¹	0.065	0.185	1.065	0.574
Crystal size/mm	0.27 × 0.35 × 0.38	0.15 × 0.23 × 0.31	0.19 × 0.31 × 0.38	0.15 × 0.31 × 0.38
Measd reflect.	36676	27382	17872	32426
Indep. reflect.	6769	3031	2771	5452
Criterion obs. refl.	<i>I</i> > 2σ(<i>I</i>)	<i>I</i> > 2σ(<i>I</i>)	<i>I</i> > 2σ(<i>I</i>)	<i>I</i> > 2σ(<i>I</i>)
<i>R</i> _{int}	0.028	0.036	0.027	0.028
<i>R</i> 1 (<i>I</i> > 2σ(<i>I</i>))	0.0518	0.0472	0.0169	0.0300
<i>wR</i> 2 (<i>I</i> > 2σ(<i>I</i>))	0.1348	0.1249	0.0432	0.0797
<i>R</i> 1 (all)	0.0676	0.0659	0.0180	0.0336
<i>wR</i> 2 (all)	0.1471	0.1361	0.0436	0.0818
Δρ max., min.	0.184, -0.248	0.189, -0.185	0.345, -0.436	0.774, -0.742

Table 2 Crystallographic details and data collection for W₂(O₂CCH₃)₂((NⁱPr)₂CC≡CPh)₂ **3B**, Mo₂(O₂CCH₃)₂((NⁱPr)₂CC≡CFc)₂ **4A**, W₂(O₂CCH₃)₂((NⁱPr)₂CC≡CFc)₂ **4B** and Mo₂(*cis*-μ-O₂C-9-anthracene)₂(η²-(NⁱPr)₂CMe)₂

	W ₂ (O ₂ CCH ₃) ₂ ((N ⁱ Pr) ₂ - CC≡CPh) ₂ 3B	Mo ₂ (O ₂ CCH ₃) ₂ ((N ⁱ Pr) ₂ - CC≡CFc) ₂ 4A	W ₂ (O ₂ CCH ₃) ₂ ((N ⁱ Pr) ₂ - CC≡CFc) ₂ 4B	Mo ₂ (<i>cis</i> -μ-O ₂ C-9-anthracene) ₂ (η ² - (N ⁱ Pr) ₂ CMe) ₂
Formula	C ₃₄ H ₄₄ N ₄ O ₄ W ₂	C ₄₂ H ₅₂ Fe ₂ Mo ₂ N ₄ O ₄ ·4C ₄ H ₈ O	C ₂₀ H ₄₀ Mo ₂ N ₄ O ₄	C ₃₄ H ₄₄ Mo ₂ N ₄ O ₄ ·3C ₄ H ₈ O
<i>M_r</i>	940.43	1268.87	592.44	980.92
Crystal system	Triclinic	Triclinic	Triclinic	Triclinic
Space group	<i>P</i> $\bar{1}$	<i>P</i> $\bar{1}$	<i>P</i> $\bar{1}$	<i>P</i> $\bar{1}$
<i>T</i> /K	150(2)	200(2)	150(2)	200(2)
<i>a</i> /Å	8.279(1)	11.135(1)	8.3023(10)	9.311(1)
<i>b</i> /Å	9.371(1)	11.862(1)	9.0596(10)	11.735(1)
<i>c</i> /Å	12.082(1)	12.321(1)	9.5252(10)	12.973(1)
<i>a</i> /°	75.741(6)	67.157(1)	68.840(4)	66.083(3)
<i>β</i> /°	71.498(6)	78.161(1)	77.080(4)	74.895(3)
<i>γ</i> /°	78.558(5)	85.503(1)	65.805(5)	68.780(5)
<i>V</i> /Å ³	854.1(2)	1468.0(2)	607.03(12)	1197.1(2)
<i>Z</i>	1	1	1	4
<i>D_c</i> /g cm ⁻³	1.828	1.435	1.621	1.361
<i>F</i> (000)	456	660	304	512
<i>λ</i> (Mo-Kα)/Å	0.71073	0.71073	0.71073	0.71073
<i>μ</i> /mm ⁻¹	6.770	0.956	1.065	0.574
Crystal size/mm	0.12 × 0.19 × 0.27	0.12 × 0.27 × 0.27	0.19 × 0.31 × 0.38	0.15 × 0.31 × 0.38
Measd reflect.	26489	40640	17872	32426
Indep. reflect.	3913	6736	2771	5452
Criterion obs. refl.	<i>I</i> > 2σ(<i>I</i>)	<i>I</i> > 2σ(<i>I</i>)	<i>I</i> > 2σ(<i>I</i>)	<i>I</i> > 2σ(<i>I</i>)
<i>R</i> _{int}	0.042	0.033	0.027	0.028
<i>R</i> 1 (<i>I</i> > 2σ(<i>I</i>))	0.0169	0.0422	0.0169	0.0300
<i>wR</i> 2 (<i>I</i> > 2σ(<i>I</i>))	0.0398	0.1174	0.0432	0.0797
<i>R</i> 1 (all)	0.0190	0.0540	0.0180	0.0336
<i>wR</i> 2 (all)	0.0404	0.1248	0.0436	0.0818
Δρ max., min.	1.152, -1.393	1.232, -0.738	0.345, -0.436	0.774, -0.742

frit and washed with 10 mL of ethanol. The solid was dried under vacuum for several hours. Overall yield: 360 mg (39.2%).

Microanalysis: found: C 63.21; H 5.26; N 3.77%. $C_{46}H_{54}Mo_2N_4O_4$ requires: C 60.13; H 5.92; N 6.10%. NMR (benzene- d_6): 1H (400 MHz) 9.25 (d, 4H, anthr.), 8.23 (s, 2H, anthr.), 7.74 (d, 4H, anthr.), 7.09 (t, 4H, anthr.), 6.95 (t, 4H, anthr.), 3.83 (septet, 4H, $CHMe_2$) 1.75 (s, 6H, N_2CMe), 1.58 (d, 12H, $CHMe_2$), 1.09 (d, 12H, $CHMe_2$). MALDI-MS: 919.2 (100%, M^+).

Computational details

Density functional theory (DFT) calculations were performed with the hybrid Becke-3 parameter exchange functional and the Lee–Yang–Parr nonlocal correlation functional (B3LYP)²² implemented in the Gaussian03 (Revision B.04) program suite²³ in conjunction with the 6-31G* basis set for all non-metal atoms and the SDD basis set with effective core potential (ECP) for all metal atoms.²⁴ The calculations were carried out on simplified models in which each isopropyl substituent was replaced with a hydrogen atom. All geometries were fully optimized at the above levels using the default optimization criteria of the program. All calculations yielded a self-consistent set of results that were verified to be a minimum on the potential energy surface (PES) by frequency analysis. Orbital analyses were completed with GaussView.²⁵ To gain insight into the electronic transitions responsible for the observed UV-vis spectrum of all compounds, time-dependent density functional theory (TD-DFT) calculations were performed using the Gaussian program suite. All calculations were run on an Itanium 2 Cluster running Linux version 2.4.18 located at the Ohio Supercomputer Center.

X-Ray crystal structure determinations

All crystals were coated with Paratone oil and mounted on a quartz fiber or a nylon cryoloop affixed to a goniometer head. All diffraction data were collected using a Nonius Kappa CCD diffractometer. All work was done at between 150 and 200 K using an Oxford Cryosystem Cryostream Cooler. Data integration was done with Denzo. Scaling and merging of data was done with Scalepack. The structures were solved by the direct or Patterson method in SHELXS-86 or SHELXS-97. A summary of crystal data is given in Tables 1 and 2 while full crystallographic details are provided in Tables S1 and S2 of the ESI.†

CCDC reference numbers 637924–637931.

For crystallographic data in CIF or other electronic format see DOI: 10.1039/b715258b

Acknowledgements

We thank the National Science Foundation for support of this work, and the Ohio Supercomputer Center for the computational resources with which the DFT calculations were performed.

References

- 1 *Multiple Bonds between Metal Atoms*, ed. F. A. Cotton, C. A. Murillo, and R. A. Walton, Clarendon Press, Oxford, 3rd edn, 2005.
- 2 (a) M. H. Chisholm and A. M. Macintosh, *J. Chem. Soc., Dalton Trans.*, 1999, 1205; (b) H. Chen and F. A. Cotton, *Polyhedron*, 1995, **14**, 2221.
- 3 F. A. Cotton, C. Lin and C. A. Murillo, *Acc. Chem. Res.*, 2001, **34**, 759.
- 4 M. H. Chisholm and N. J. Patmore, *Acc. Chem. Res.*, 2007, **40**, 17.
- 5 M. H. Chisholm, *Proc. Natl. Acad. Sci. U.S.A.*, 2007, **104**, 2563.
- 6 A. R. Sadique, M. J. Heeg and C. H. Winter, *J. Am. Chem. Soc.*, 2003, **125**, 7774.
- 7 B. S. Lim, A. Rahtu, J.-S. Park and R. G. Gordon, *Inorg. Chem.*, 2003, **42**, 7951.
- 8 M. P. Coles, D. C. Swenson and R. F. Jordan, *Organometallics*, 1997, **16**, 5183.
- 9 S. Dagonne and R. F. Jordan, *Organometallics*, 1999, **18**, 4619.
- 10 B. E. Bursten, M. H. Chisholm, R. J. H. Clark, S. Firth, C. M. Hadad, A. M. Macintosh, P. J. Wilson, P. M. Woodward and J. M. Zaleski, *J. Am. Chem. Soc.*, 2002, **124**, 3050.
- 11 D. L. Lichtenberger, M. A. Lynn and M. H. Chisholm, *J. Am. Chem. Soc.*, 1999, **121**, 12167.
- 12 M. H. Chisholm, J. S. D'Acchioli, B. D. Pate, N. J. Patmore, N. S. Dalal and D. J. Zipse, *Inorg. Chem.*, 2005, **44**, 1061.
- 13 (a) G.-L. Xu, R. J. Crutchley, M. C. DeRosa, Q.-J. Pan, H.-X. Zhang, X. Wang and T. Ren, *J. Am. Chem. Soc.*, 2005, **127**, 13354; (b) G.-L. Xu, M. C. DeRosa, R. J. Crutchley and T. Ren, *J. Am. Chem. Soc.*, 2004, **126**, 3728.
- 14 M. J. Byrnes, M. H. Chisholm, J. C. Gallucci, Y. Liu, R. Ramnauth and C. Turro, *J. Am. Chem. Soc.*, 2005, **127**, 17343.
- 15 S. Jones, J. C. C. Atherton, M. R. J. Elsegood and W. Clegg, *Acta Crystallogr., Sect. C*, 2000, **56**, 881.
- 16 M. J. Byrnes, M. H. Chisholm, D. F. Dye, C. M. Hadad, P. D. Pate, P. J. Wilson and J. M. Zaleski, *Dalton Trans.*, 2004, 523.
- 17 For a related reaction, see: M. H. Chisholm, A. J. Epstein, J. C. Gallucci, F. Fiel and W. Pirkle, *Angew. Chem., Int. Ed.*, 2005, **44**, 6537.
- 18 R. H. Cayton, M. H. Chisholm, J. C. Huffman and E. B. Labkovsky, *J. Am. Chem. Soc.*, 1991, **113**, 8709.
- 19 T. A. Stephenson, E. Banister and G. Wilkinson, *J. Chem. Soc.*, 1964, 2538.
- 20 D. J. Santure, J. C. Huffman and A. P. Sattelberger, *Inorg. Chem.*, 1985, **24**, 371.
- 21 M. J. Byrnes, M. H. Chisholm, R. J. H. Clark, J. C. Gallucci, C. M. Hadad and N. J. Patmore, *Inorg. Chem.*, 2004, **43**, 6334.
- 22 A. D. J. Becke, *Chem. Phys.*, 1993, **98**, 5648.
- 23 M. J. Frisch, G. W. Trucks, H. B. Schlegel, G. E. Scuseria, M. A. Robb, J. R. Cheeseman, J. A. Montgomery, Jr., T. Vreven, K. N. Kudin, J. C. Burant, J. M. Millam, S. S. Iyengar, J. Tomasi, V. Barone, B. Mennucci, M. Cossi, G. Scalmani, N. Rega, G. A. Petersson, H. Nakatsuji, M. Hada, M. Ehara, K. Toyota, R. Fukuda, J. Hasegawa, M. Ishida, T. Nakajima, Y. Honda, O. Kitao, H. Nakai, M. Klene, X. Li, J. E. Knox, H. P. Hratchian, J. B. Cross, V. Bakken, C. Adamo, J. Jaramillo, R. Gomperts, R. E. Stratmann, O. Yazyev, A. J. Austin, R. Cammi, C. Pomelli, J. Ochterski, P. Y. Ayala, K. Morokuma, G. A. Voth, P. Salvador, J. J. Dannenberg, V. G. Zakrzewski, S. Dapprich, A. D. Daniels, M. C. Strain, O. Farkas, D. K. Malick, A. D. Rabuck, K. Raghavachari, J. B. Foresman, J. V. Ortiz, Q. Cui, A. G. Baboul, S. Clifford, J. Cioslowski, B. B. Stefanov, G. Liu, A. Liashenko, P. Piskorz, I. Komaromi, R. L. Martin, D. J. Fox, T. Keith, M. A. Al-Laham, C. Y. Peng, A. Nanayakkara, M. Challacombe, P. M. W. Gill, B. G. Johnson, W. Chen, M. W. Wong, C. Gonzalez and J. A. Pople, *GAUSSIAN 03 (Revision B.04)*, Gaussian, Inc., Wallingford, CT, 2003.
- 24 Æ. Frisch, M. J. Frisch and G. W. Trucks, *Gaussian 03 User's Reference*, Gaussian, Inc., Wallingford, CT, 2003.
- 25 Æ. Frisch, R. D. Dennington and T. A. Keith, *GaussView Reference*, Gaussian, Inc., Wallingford, CT, 2003.